Electron-electron scattering and phase fluctuations in superconducting films

Soon-Gul Lee* and Thomas R. Lemberger
Department of Physics, Ohio State University, Columbus, Ohio 43210
(Received 4 April 1989)

The effects of weak disorder on superconducting aluminum films are studied over temperatures $0.4T_c \leq T \leq 0.98T_c$ and resistances per square of $1.7 \leq R_\square \leq 22\ \Omega$. The primary effects of disorder are found to be disorder-enhanced electron-electron scattering and thermal phase, or supercurrent fluctuations, both of which cause pair-breaking effects. This conclusion is drawn from measurement of the low-voltage resistance of low-resistance superconductor–insulator–normal-metal (SIN) tunnel junctions with aluminum as the S electrode. The effective pair-breaking rates from both processes, evaluated at T_c, increases linearly with $R_\square$, in semiquantitative agreement with model calculations. The electron-electron scattering rate decreases very rapidly as T decreases below T_c, in agreement with theory. The pair-breaking rate from phase fluctuations decreases roughly linearly with decreasing temperature. Although distinct effects, phase fluctuations, and electron-electron scattering share a common origin in electron-density fluctuations, which are enhanced by disorder. A microscopic theory of disordered superconductors incorporating both electron-electron scattering and thermal phase fluctuations is needed.

I. INTRODUCTION

Recently we found that the dominant effects of disorder on the microscopic properties of superconducting films arise from pair-breaking effects of thermal phase fluctuations and from electron-electron (*e-e*) scattering. The phase of the superconducting order parameter fluctuations in space and time in response to thermal fluctuations in the local electrochemical potential; fluctuations in the gradient of the phase represent fluctuations in the local supercurrent density. The effects were observed in weakly disordered superconducting Al films[1,2] from measurements of the low-voltage resistance of low-resistance superconductor–insulator–normal-metal (SIN) tunnel junctions. Quantitative agreement with model calculations was found for limited values of resistance per square ($R_\square \sim 1\ \Omega$) of the Al film and for temperatures T greater than about $0.7T_c$. The present paper reports a systematic extension of this investigation to $1.7 \leq R_\square \leq 22\ \Omega$ and to temperatures down to $0.4T_c$.

Much previous work on disordered superconductors[3–9] has focused on the effects of disorder on the transition temperature and the critical magnetic field. Theoretical[10,11] and experimental[12–15] work has led to the picture that weak disorder in the normal state enhances the inelastic *e-e* scattering rate. Extrapolating this to below T_c, one could expect *e-e* scattering to persist and have important effects such as broadening the singularity in the BCS density of states. (Of course, disorder also may change the mechanical properties of the film, e.g., the Debye frequency, or change the electronic properties, e.g., the density and effective mass of the conduction electrons. The effects of these changes on superconducting properties are in some sense "trivial" since they shift T_c without changing qualitatively the microscopic parameters such as the density of states.[16]) Measurements in the normal state[12–15] have verified quantitative predictions for the *e-e* scattering rate above T_c, but only limited attempts have been made to measure the rate below T_c.[17,18] The major results of the present investigation are the discovery of the importance of phase fluctuations, and determination of the dependence of both the phase fluctuation and *e-e* pair-breaking rates on T and on $R_\square$ for relatively weak disorder.

In this investigation, we measure the low-voltage resistance R_j of low-resistance Al-AlO_x-Cu tunnel junctions as a function of temperature and of the supercurrent flowing in the Al film. The supercurrent is generated both by direct application from a current source and by induction with a magnetic field parallel to the Al film. The quantitative accuracy of this method for determining electron scattering rates in superconductors has been demonstrated by detailed measurements on SIN junctions involving superconducting Sn and SnIn films,[19] interpreted with the theory given in Ref. 20.

The concept behind our technique is different from conventional tunneling measurements on SIN junctions because here the junction resistance is so low that the quasiparticle disequilibrium generated in the superconductor by the measuring current is responsible for a substantial portion of the measured junction resistance. Thus we can study scattering processes associated with quasiparticle relaxation from measurements of R_j. The particular disequilibrium is often called a quasiparticle charge imbalance.[21] For a fixed tunneling current, its magnitude and temperature dependence reflect the magnitude, energy, and explicit temperature dependences of the various processes that contribute to charge-imbalance relaxation. (For the purposes of this paper, we define pair-breaking processes to be any processes that relax a

 ©1989 The American Physical Society

charge imbalance.[22] This defines as pair breaking all inelastic scattering processes; elastic scattering from lattice defects and impurities when the order parameter is anisotropic due to supercurrents or intrinsic anisotropy; and scattering from magnetic impurities.) We can isolate experimentally the charge-imbalance part R_{Q^*} of the total junction resistance R_j because R_{Q^*} is very sensitive to the presence of a supercurrent in the superconducting film. The supercurrent shortens the net relaxation time by inducing anisotropy in the order parameter and thereby activating pair breaking from elastic scattering.

In brief, the theoretical analysis involves two steps. The first is to determine the nonequilibrium distribution function for the quasiparticles in the superconductor. This is done by solving the appropriate Boltzmann-like equation.[20] This equation determines the distribution function of quasiparticles in energy by balancing the rate of generation of quasiparticles by the electrochemical potential drop V_j across the junction against the net relaxation rate due to *e-e* scattering, elastic scattering from defects and nonmagnetic impurities in the presence of gap anisotropy induced by thermal supercurrent (phase) fluctuations and an externally imposed supercurrent, and the proximity coupling between the superconducting and normal films comprising the junction. The second step is to use the distribution function for the quasiparticles and the superconducting density of states, appropriately modified by pair breaking, to calculate the tunneling current I_j through the junction, and thus the junction resistance $R_j = V_j / I_j$. The important fitting parameters are the magnitudes of the *e-e* and phase-fluctuation pair-breaking rates at T_c. The explicit dependences of these rates on energy and on T are determined by model calculations. In the end the accuracy of the fit to the data at all temperatures and applied supercurrents supports the validity of the model calculations.

As described below, the measured values at T_c of both the *e-e* pair-breaking rate and the phase-fluctuation pair-breaking rate increase with $R_\square$. The magnitude of the *e-e* rate at T_c agrees with the results of magnetoresistance measurements in the normal state[13,15] but disagrees with the values obtained by a microwave technique.[17] Below T_c the *e-e* scattering rate decreases very rapidly.[16,23] The pair-breaking rate from thermal phase fluctuations has a roughly linear temperature dependence in agreement with a simple model calculation presented below.

II. EXPERIMENTAL DETAILS

The samples are low-resistance Al-AlO_x-Cu tunnel junctions, in which the Al films are slightly disordered. The sample configuration and wiring diagram are illustrated in Fig. 1. All the films are vapor deposited *in situ* from resistively heated sources through mechanical aperture masks onto glass substrates which are at room temperature. To improve the uniformity of current distribution in the superconducting Al film and thus to maximize the measured critical current, junctions are built on thick anodized Nb ground planes. Nb ground planes are made by depositing about 0.5-μm-thick Nb films on glass slides

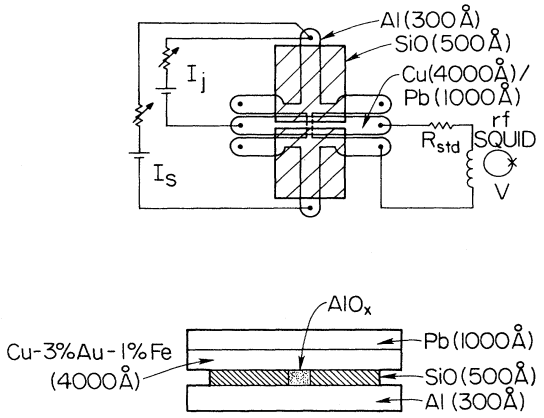

FIG. 1. Sample configuration and wiring diagram.

by dc sputtering and anodizing them in a solution prepared from 280 ml of water, 420 ml of ethylene glycol and 58 g of ammonium pentaborate with a large area stainless steel blade as a cathode plate. The anodization current used is 0.5 mA/cm^2 of Nb films and anodization is finished at 1500 Å. Niobium oxide grows at the rate of 23 Å/V (about 8 Å/V of Nb).

The thickness of the Al films is about 300 Å and the width is about 300 μm. The residual resistance per square $R_\square$ of the Al film is controlled by the O_2 partial pressure in the deposition system during evaporation, typically $\sim 1\times10^{-5}$–6×10^{-5} torr, and by the deposition rate of $\sim$4–5 Å/sec. These parameters give $R_\square = \sim 1$–25 Ω. The thin insulating layer in the junction is made by oxidizing the Al films in an atmosphere of 5×10^{-5} to 5×10^{4} torr O_2 for a minute or two just after the deposition. The junction area is defined by masking the Al films by a 500-Å SiO layer except for a 300 μm length in the middle. With these processes we obtain junction resistances ranging from 0.1 to 5 mΩ near T_c.

A superconducting quantum interference device (SQUID) is used in a nulling feedback mode to measure the junction voltage. The noise in the measurement is $\sim$10 pV for a 10-Hz bandwidth. For stability, mercury batteries are used for current sources for the junction bias current and the applied supercurrent in the Al film. rf noise is suppressed by doing measurements in a rf-shielded room and reduced further by the use of a superconducting Pb bag on the probe. To avoid geomagnetic fields a dual-layered μ-metal shield is put around the Dewar. The maximum ambient flux density measured inside the Dewar is less than 10 mG at room temperature, small enough to have no effect on our results. Measurements are done from 0.65 K to T_c with a ^{3}He probe.

The junction resistance R_j is measured as a function of temperature, transport supercurrent applied in the superconducting film, and magnetic field parallel to the film. R_j is determined from the current-voltage (I-V) characteristic at low voltages. Because the intrinsic resistances of the junctions are only about 1 mΩ, the voltage is always kept less than 100 nV to ensure that heating is negligible and the current-voltage characteristic is linear.

Measurement of R_j as a function of the transport supercurrent I_s in the superconducting Al film is made by fixing the junction current I_j and then measuring the change in the junction voltage V_j as a function of I_s. The additional supercurrent in the Al film due to the junction bias current is always negligible. We check that the Al film is superconducting for the range of supercurrents used here by measuring V_j versus I_s for $I_j=0$. Any data obtained in the resistive state of the Al film $[V_j(I_s,I_j=0)\neq 0]$ is discarded.

The applied supercurrent in the Al film is uniform across the thickness because twice the magnetic penetration depth $2\lambda > 5000$ Å is much larger than the film thickness $d \sim 300$ Å. The uniformity of the current density across the width of the film is improved by the use of superconducting Nb ground planes. With the underlying ground plane, the measured critical current of the Al film is about 30% of the calculated Ginzburg-Landau critical current which is large enough to obtain sufficient $R_j(T)$ versus I_s data for theoretical analysis, i.e., at least twice the current at the inflection point of the $R_j(I_s)$ curve whose importance will be demonstrated below.

Measurement of R_j as a function of magnetic field is made by fixing I_j, then measuring V_j as a function of magnetic field $B_\parallel$ parallel to the film. The value of $B_\parallel$ is determined from the current in the magnet coil. The effect of a magnetic field should be the same as that of an applied supercurrent since the magnetic field simply induces diamagnetic screening supercurrents.[24] For uniformly thin, $d \ll 2\lambda$, homogeneous films, the only difference is that the current distribution is nonuniform in the case of applied fields, being 0 in the center plane of the film and maximal near the film surfaces. The maximum applied field is about 200 G. Larger magnetic fields result in flux trapping and the R_j versus $B_\parallel$ curves become asymmetric and irreversible.

Although measurements of R_j versus I_s and R_j versus $B_\parallel$ in principle contain the same information, they serve as checks on each other because of the different distributions of supercurrent density. One result of the difference is that the calculated pair-breaking rate from a measured transport supercurrent is inversely proportional to the film thickness d, for given $R_\square$, while that of a measured magnetic field is proportional to d.[18,25] Thus we expect that inevitable minor sample nonidealities, such as thickness variations, may cause quantitative discrepancies between the two measurements, but should not result in qualitative differences. As discussed below, we find excellent qualitative agreement with generally small quantitative discrepancies.

III. EXPERIMENTAL RESULTS AND DISCUSSION

A. Experimental results and data analysis

Measured sample parameters are listed in Table I. Before discussing the measurements, we compare some important length scales to put our samples into context. The electron mean free paths l for all samples are much shorter than the clean limit coherence length $\xi_0=\hbar V_F/\pi\Delta_0 \cong 16\,000$ Å (Ref. 26). Thus the films are in the dirty limit and appropriate expressions must be used for the Ginzburg-Landau coherence length $\xi(T)$ and magnetic penetration depth $\lambda(T)$.[25] Since the electron thermal coherence length $(D\hbar/k_BT)^{1/2}$ is larger than the film thickness, *e-e* interactions are effectively two dimensional.[13,15,27]

We now move on to describe and interpret our measurements of junction resistance R_j as a function of temperature and of supercurrent and magnetic field. The important parameters, such as the values of the various scattering rates at T_c, are determined from detailed fits to the data of numerical solutions of the theory described in detail in Refs. 1, 19, and 20. In the present paper, we give a qualitative description that illustrates the underlying concepts and clarifies what features of the data determine each parameter. We begin by appealing to several useful theoretical results that are strictly valid only near T_c, but are qualitatively accurate for lower temperatures.

First, R_j can be written as the sum of two components:

$$R_j(T)=R_{\rm eq}(T)+R_{Q*}(T)\ , \tag{1}$$

where $R_{\rm eq}(T)$ is the "equilibrium" junction resistance that has the T dependence of high-resistance junctions, in which the "nonequilibrium" resistance R_{Q*} is negligibly small. R_{Q*} is due to the nonequilibrium charge imbal-

TABLE I. Sample parameters. Samples are arranged in the order of resistance per square.

Sample	d (Å)	w[a] (μm)	l[b] (Å)	R[c] (Ω)	T_c (K)	R_N (mΩ)	$1/\tau_{\rm tun}$ (10^8 s^{-1})
1	300	286	77.5	1.72	1.470	1.67	0.35
2	422	300	41.0	2.31	1.519	0.16	3.1
3	343	300	49.3	2.37	1.480	1.0	0.58
4	301	300	21.6	6.15	1.808	0.165	3.2
5	303	286	18.0	7.2	1.800	3.25	0.18
6	303	314	15.3	8.62	1.920	1.26	0.43
7	300	315	11.6	11.5	1.905	4.44	0.12
8	300	300	6.0	22.3	2.070	1.25	0.47

[a] w is width of Al film.

[b] l is electron mean free path of Al film calculated from $\rho l = 4\times 10^{-16}\ \Omega\,{\rm m}^2$ (Ref. 33).

[c] $R_\square$ is resistance per square of Al film.

ance generated by the current used to measure R_j. At low temperature, $R_j \sim R_{eq}$, and both increase very rapidly as T decreases due to an exponential decrease of excitation probability associated with the energy gap. Near T_c, R_{eq} approaches the intrinsic junction resistance R_N, but R_{Q^*} diverges proportional to the charge-imbalance relaxation time τ_{Q^*} and hence R_j diverges. $R_{Q^*}(T)$ is approximately proportional to the relaxation time τ_{Q^*}:[19,28]

$$R_{Q^*}(T) \cong R_{eq}(T) \frac{\tau_{Q^*}}{\tau_{tun}} . \quad (2)$$

In Eq. (2), $1/\tau_{tun}$ is the rate at which an electron at the Fermi surface tunnels through the insulator from the superconductor to the normal metal,[28,29] and it represents the pair-breaking proximity effect between the N and S films through the insulator. It is defined as $\tau_{tun} \equiv 2N(0)e^2\Omega R_N$, where $2N(0)$ is the volume density of states of the S film and Ω is the volume of the S film in the junction area. $2N(0) = 3.48 \times 10^{28}/\text{eV}\,m^3$ for Al.[26,30] Finally, $1/\tau_{Q^*}$ is related to the intrinsic pair-breaking rates, which are the focus of this investigation, and the extrinsic pair-breaking current through[31,32]

$$\frac{1}{\tau_{Q^*}} \cong \frac{\pi\Delta}{2k_BT}\left[\frac{1}{2\tau_{in}}\left[\frac{1}{2\tau_{in}}+\frac{1}{\tau_s}\right]\right]^{1/2} . \quad (3)$$

For the present measurements $1/2\tau_{in} = 1/2\tau_{e\text{-}e} + 1/2\tau_{tun}$ is the sum of the e-e and tunneling pair-breaking rates and $1/\tau_s = 1/\tau_{s,ext} + 1/\tau_{SCF}$ is the sum of the elastic pair-breaking rates due to applied supercurrents (extrinsic) and supercurrent fluctuations. From Eq. (3), R_{Q^*} diverges as k_BT_c/Δ near T_c. The appearance of this divergence in the data is the signature of charge imbalance.

Figure 2 shows $R_j(T)$ for one of our samples. The charge-imbalance contribution to the junction resistance is substantial (about 10% near T_c from R_j versus I_s data which will be chosen below), but it is almost invisible on the scale of Fig. 2 except for the small rise very near T_c. Two important parameters can be read from this data immediately. The minimum value of $R_j(T)$, which occurs close to T_c, is approximately equal to the intrinsic resistance R_N of the junction, so that the tunneling rate $1/\tau_{tun}$ is determined. Also, the divergence of R_j determines T_c to within about 10 mK.

While data on R_j versus T yield reasonably accurate values for R_N, $1/\tau_{tun}$, and T_c, they are insufficient to determine the intrinsic rates of interest here. The key measurements to determine $1/\tau_{e\text{-}e}(T_c)$ and $1/\tau_{SCF}(T_c)$ are R_j versus I_s and R_j versus $B_\parallel$. The concept is as follows. The intrinsic processes of e-e scattering and thermal phase fluctuations determine the magnitude of R_{Q^*} since they determine τ_{Q^*} [Eqs. (2) and (3)]. An extrinsic pair breaker, i.e., I_s or $B_\parallel$, reduces the relaxation time τ_{Q^*}, and thence R_{Q^*}. When the extrinsic pair-breaking rate $1/\tau_{s,ext}$ equals the intrinsic rate, R_{Q^*} is reduced by about half and this point can, in principle, be used to estimate the intrinsic rate. Unfortunately one does not know where "half" is unless the entire curve is measured out to $R_{Q^*} \sim 0$, and this is usually not possible. A more convenient measure of the intrinsic pair-breaking rate can be obtained from the value of $1/\tau_{s,ext}$ at the inflection point in R_j versus I_s or $B_\parallel$. At the inflection point, the extrinsic rate is approximately half of the intrinsic rate. [This relation can be obtained from Eqs. (1)–(3) if $1/\tau_s$ is the sum of an intrinsic rate and an extrinsic rate proportional to I_s^2 or $B_\parallel^2$, and R_{eq} and Δ are not affected by the extrinsic pair breaker. This last condition breaks down very close to T_c where the dependence of Δ on $1/\tau_{s,ext}$ becomes important.] Although the inflection point is not sharply defined, and hence accurate values of $1/\tau_{e\text{-}e}(T_c)$ and $1/\tau_{SCF}(T_c)$ are obtained in the end from detailed comparison of data with numerically calculated curves, we fill focus on the inflection points in the discussion to obtain a quick qualitative insight into the data.

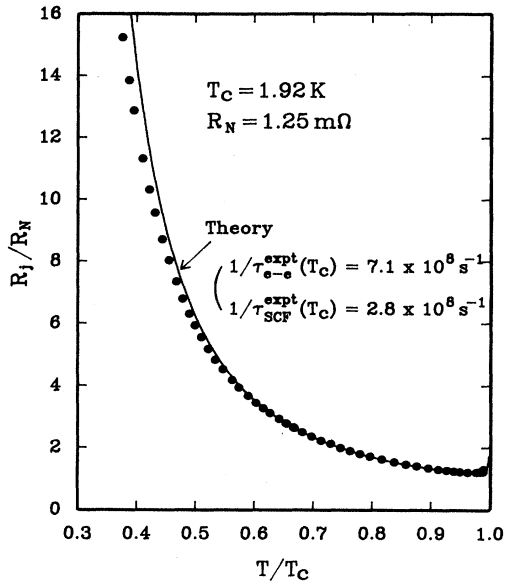

FIG. 2. Junction resistance as a function of temperature for sample 6. The rates at T_c were obtained from the best fit of theory to both $R_j(T)$ and $R_j(I_s)$ data.

Figure 3 shows the fractional change of junction resistance $\delta R_j/R_j$ versus $I_s/I_c(0)$, where $I_c(0)$ is the theoretical critical current at $T=0$ calculated from the measured sample parameters from[33]

$$I_c^2(0) = 2.562dw^2 2N(0)(k_BT_c)^3/\hbar R_\square . \quad (4)$$

The change $\delta R_j(T,I_s)$ is mostly from the decrease of $R_{Q^*}(T)$. R_{eq} changes only when $1/\tau_{s,ext}$ approaches $\Delta/\hbar$, which is much larger than the intrinsic pair-breaking rate. The pair-breaking rate is related to the applied supercurrent through the dirty-limit expression:[24]

$$\frac{1}{\tau_{s,ext}} = \frac{Dp_s^2}{2\hbar^2} = \frac{2\gamma^2 R_\square}{\pi^4 2N(0)(k_BT_c)^2 dw^2}\frac{n_s(0)^2}{n_s(T)^2}I_s^2 , \quad (5)$$

where D is the electron diffusion constant, $p_s = 2mv_s$ is the superfluid momentum, v_s is the superfluid velocity,

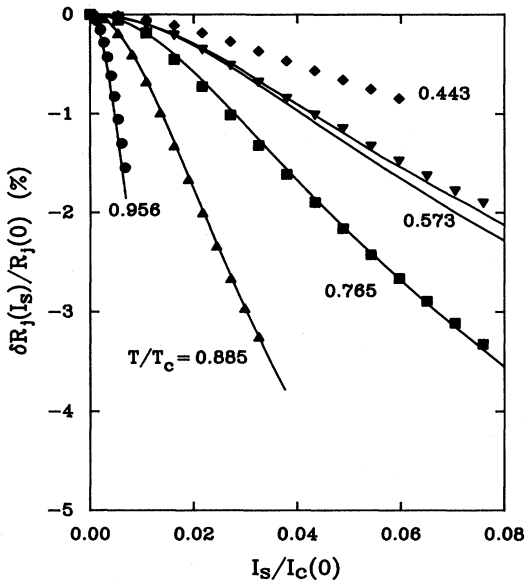

FIG. 3. Fractional change of junction resistance as a function of applied supercurrent in the Al film for sample 6. Theory curves were calculated with the same rates shown in Fig. 2.

and $\pi/\gamma = 1.764$. n_s is the density of superconducting electrons. For the second equality in Eq. (5) the free electron relation $1/\rho = 2N(0)e^2D$ was used, where ρ is the residual resistivity.

The theoretical curves in Figs. 2 and 3 are calculated from a Boltzmann-like equation for the quasiparticle distribution function[20] in which generation of excitations from tunneling at each energy level is balanced against relaxation due to *e-e* scattering, phase fluctuations, and the proximity effect. Because the full integral form of the Boltzmann equation is used, rather than a relaxation approximation, the only adjustable parameters are the magnitudes of the *e-e* and phase-fluctuation rates at T_c.

The calculated curves in Figs. 2 and 3 agree with data very well both qualitatively and quantitatively from T_c down to $0.5T_c$. In Fig. 3 especially note that the calculated inflection points occur at the same values of $I_s/I_c(0)$ as in the data, within $\pm 10\%$ (actual data are continuous curves from an XY chart recorder but here shown in symbols just to clearly distinguish them from theory curves). The significance of the inflection point allows us to understand the data at $0.443T_c$. There, the calculation overestimates $\delta R_j/R_j$ by a factor of almost 2 but accurately reproduces the value of $1/\tau_{s,\mathrm{ext}}$ at the inflection point. Our interpretation of this discrepancy is that there are weak spots in the junction insulator. Weak spots decrease R_{eq} because the gap is reduced in the superconductor by the proximity coupling to the normal metal. Weak spots decrease R_{Q*} because the charge imbalance is reduced by diffusion of quasiparticles away from the weak spot. The effect of weak spots is enhanced at low T because the resistance through the strong parts of the junction becomes very large so current focuses into weak spots. Now, if our physical interpretation of the inflection point in terms of changing the charge-imbalance relaxation time with the applied supercurrent is correct, then the inflection point in the data should occur at the same extrinsic pair-breaking rate as in the calculation, regardless of the magnitude of R_{Q*}, and this is what is observed.

To emphasize the importance of including phase fluctuations as well as *e-e* scattering in the theory, Fig. 4 shows the data from Fig. 3 with curves calculated without phase fluctuations but with an *e-e* scattering rate magnified by a factor of 4 to match the data at $0.956T_c$. As T decreases below $0.956T_c$, in the calculated curves the inflection points occur at a smaller supercurrent than is observed, indicating that the *e-e* rate in the calculation decreases much more rapidly than the intrinsic relaxation rate in the film. (Calculations presented below quantify the rapid decrease in the *e-e* rate just below T_c.) Considering that $1/\tau_{s,\mathrm{ext}} \propto I_s^2$, the calculated intrinsic rate at $0.573T_c$ is smaller than the measured rate by a factor of $\sim 5-6$.

Because of their different dependences on temperature, the contributions of *e-e* scattering and phase fluctuations to the total intrinsic pair-breaking rate can be separated in the numerical fits to the data. Our calculations show that while the electron-electron scattering rate drops very sharply as T decreases, the phase-fluctuation rate decreases linearly with decreasing T, as will be demonstrated in Sec. III B. At low temperatures, phase fluctuations dominate, and the pair-breaking rate due to fluctuations is determined with precision. With the fluctuation rate determined, the *e-e* rate is determined by optimizing the fits to data near T_c. Fits comparable in quality to those

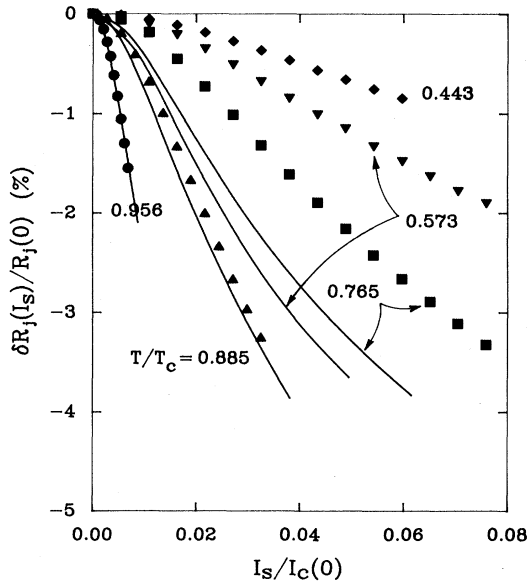

FIG. 4. Same data as in Fig. 3, but with theory curves calculated with $1/\tau_{\mathrm{SCF}}(T_c) = 0$ and with $1/\tau_{e\text{-}e}(T_c) = 2.8 \times 10^9/\mathrm{s}$, i.e., four times larger than expected from Eq. (7) as is needed to match the data at $T/T_c = 0.956$.

shown in Figs. 2 and 3 were found for all temperatures for all of the junctions reported here, that is, for all high-quality junctions as judged by a rapid rise in R_j at low temperatures.

Uncertainties associated with the rates shown in Fig. 2 are as follows. The sum of the pair-breaking rates, $1/\tau_{SCF}(T_c)+1/2\tau_{e\text{-}e}(T_c)$, is determined to $\pm 10\%$. The uncertainty in the *e-e* rate $1/\tau_{e\text{-}e}(T_c)$ alone is $\pm 20\%$; for the phase (supercurrent) fluctuation rate $1/\tau_{SCF}(T_c)$ alone, $\mp 10\%$. There is a large uncertainty in the fitted value of the *e-e* scattering rate because the rate decreases so rapidly below T_c that it is overshadowed by the larger phase-fluctuation relaxation rate over the accessible experimental range. For all the samples studied uncertainties of fitted rates have similar magnitudes.

As discussed in the next section, physical considerations lead us to expect $1/\tau_{e\text{-}e}(T_c)$ and $1/\tau_{SCF}(T_c)$ to be proportional to $R_\square$ and T_c. To illustrate the dependence of these rates on disorder, Fig. 5 shows the fitted values of these rates, normalized to T_c, versus $R_\square$ of the Al film at 4.2 K. $R_\square$ ranges from 1 to 20 Ω per square, which is still the weak disorder limit, $R_\square \ll 4$ kΩ. Both rates are approximately linear in $R_\square$. The phase-fluctuation rate seems to increase more slowly than linearly; $R_\square^{2/3}$ is a better fit. Figure 5 summarizes the most important experimental results of this paper.

Some important assumptions implicit in the theory have been checked experimentally. The analysis of R_j versus I_s assumes a uniform supercurrent density J_s in a uniformly thin Al film. However, J_s is larger near the edges of the Al film than at the middle because the width w of the films is much larger than the transverse penetration depth $\lambda_t=\lambda^2/d$ (Ref. 34). Moreover, all films have

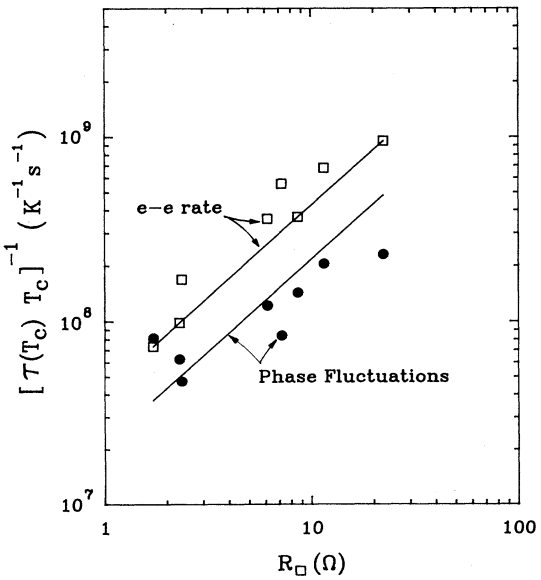

FIG. 5. Fitted values of $1/\tau_{SCF}(T_c)$ and $1/\tau_{e\text{-}e}(T_c)$ vs $R_\square$ for eight samples studied. Note that both electron-electron scattering and fluctuation terms increase roughly linearly with $R_\square$.

inevitably some forms of inhomogeneity, such as thickness variations. The following independent experimental tests indicate that both of these considerations are negligible.

First, measurements of the effect of a supercurrent on high-resistance SIN junctions, with the same geometry and materials are those reported here, are in excellent agreement with calculations that assume a uniform supercurrent density.[35] In these measurements, only R_{eq} is observed since R_{Q^*} is negligibly small in comparison. The theory for R_{eq} versus I_s has been long established, and any discrepancy would have indicated the need for a more precise physical model of the superconducting film. Apparently J_s is very close to its average value I_s/wd throughout most of the superconducting film because the increase in J_s occurs over a very small range ($\sim\lambda_t \simeq 5$ $\mu m \ll w$) near the edges and does not draw much current away from the rest of the film.

Second, we have probed indirectly the importance of nonuniformities in the films by comparing results with a directly applied supercurrent to results with a supercurrent induced by a magnetic field parallel to the superconducting Al film. The field was oriented along the length of the Al film, so the induced currents flowed across the top of the film, around the edges, then back across the bottom surface. According to theory, the pair-breaking rate is proportional to the spatial average of J_s^2 (Ref. 24) for films with $d \ll \lambda$. For homogeneous, uniformly thin films, the different spatial distribution of J_s should be unimportant; the effect of the field should be the same as an applied supercurrent when the data are expressed in terms of the extrinsic pair-breaking rate.

Figure 6 shows for $R_j(B_\parallel)$ and $R_j(I_s)$ along with theory curves calculated with both electron-electron scattering and phase fluctuations for sample 3. The pair-breaking rate due to the applied parallel field $B_\parallel$ was calculated from[24,25]

$$1/\tau_{s,\text{ext}}=\frac{De^2B_\parallel^2d^2}{6\hbar^2}=\frac{B_\parallel^2 d}{12N(0)R_\square\hbar^2}\ , \tag{6}$$

where free electron relations were used for the second equality. We used the film thickness d, which is known to about $\pm 15\%$ for these thin films, as a fitting parameter to get the excellent agreement shown in Fig. 6. Clearly there is no qualitative difference between applied and induced supercurrents, despite the different spatial distribution of currents. Quantitative discrepancies were occasionally observed. In the worst case, the fitted film thickness was 40% larger than the measured value, which was outside of uncertainty. We do not know the reason for this. However, we conclude that the qualitative, and usually quantitative, agreement between measurements with applied and induced supercurrents supports our assumptions of uniform films and supercurrent density in the analysis. We believe that the data taken with an applied supercurrent are more accurate because of the quantitative accuracy and reproducibility of a previous study of Sn and SnIn films[19] using the same technique as the present study, and because of the quantita-

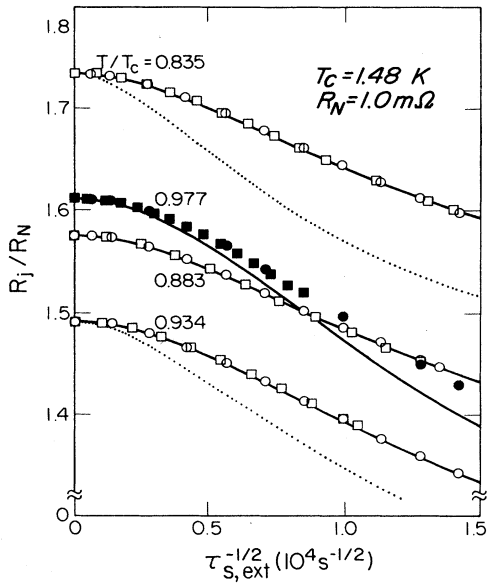

FIG. 6. Junction resistance as function of square root of extrinsic pair-breaking rate, where the pair breaking comes from both supercurrents (□) and magnetic fields parallel to the Al film (○) for sample 3. Horizontal axis was calculated using Eqs. (5) and (6), with film thickness d as a fitting parameter for comparison of the two different sets of data. Theory curves were calculated with $1/\tau_{SCF}(T_c)=0.7\times10^8$/s and $1/\tau_{e\text{-}e}(T_c)=2.5\times10^8$/s.

tive success of measurements of the effect of a supercurrent on high-resistance SIN junctions[35] mentioned above.

B. Model calculations

1. Electron-electron scattering

Based on the currently accepted model of disordered metal films,[10,11,16,23] disorder-enhanced e-e scattering arises from the coupling of single electron excitations to electric field fluctuations generated thermally by electron-density fluctuations, that is, thermally excited damped plasmons. Even though the plasma frequency is very high, there is a finite spectral density at low frequencies from damping due to elastic scattering of electrons. In two dimensions the effective electron-plasmon coupling function for e-e scattering, analogous to the electron-phonon coupling function, is $\alpha^2F(\omega)=e^2R_\square/8\pi^2\hbar$ (Ref. 10). Note that it is independent of energy and increases linearly with $R_\square$. Above T_c, this function gives an inelastic e-e scattering rate approximately linear in T and $R_\square$ (Refs. 10–15).

In the Boltzmann equation, the e-plasmon coupling function simply adds to the (here negligible) electron-phonon coupling function in the collision integral. (Details of the integral, e.g., coherence factors, thermal occupation factors, etc., are explained in Refs. 20 and 36.) Unlike the calculation of the phase-breaking rate in the normal state which determines the localization of electron wave functions,[10,11] there is no problem with convergence because the coherence factor that governs charge-imbalance relaxing processes cuts off the divergence at low energies. The temperature dependence of the net e-e scattering rate is determined from its energy dependence and the Boltzmann equation.

Although the actual fitting parameter is the coupling function α^2F, for comparison with rates determined with other techniques it is useful to define a characteristic e-e scattering rate for charge-imbalance relaxation, as was done in Ref. 1:

$$\frac{1}{\tau_{e\text{-}e}^{\text{theor}}(T_c)}=28\pi\zeta(3)\alpha^2F\frac{k_BT_c}{\hbar}\simeq4.3\times10^7R_\square T_c\ , \tag{7}$$

in $(\Omega\,\mathrm{K\,s})^{-1}$, where $\zeta(3)\cong1.202$. In Table I and the figures, the fitted values $1/\tau_{e\text{-}e}^{\text{expt}}(T_c)$ were calculated with the fitted α^2F and Eq. (7). The theoretical values of $1/\tau_{e\text{-}e}^{\text{theor}}(T_c)$ were calculated from Eq. (7) with the measured value of $R_\square$. The definition, Eq. (7), was chosen so that the calculated charge-imbalance relaxation rate near T_c is[31,37]

$$\frac{1}{\tau_{Q^*}}\cong\frac{\pi\Delta}{4k_BT_c\tau_{e\text{-}e}^{\text{theor}}(T_c)}\ , \tag{8}$$

when e-e scattering is the dominant charge-imbalance relaxation mechanism, in analogy to the result when electron-phonon scattering dominates.[31] Equation (7) is very similar to, but not identical to, the phase-breaking rate familiar in localization studies,[10–15] which involves a different average over energy transfers.

The upper solid line in Fig. 5 was calculated from Eq. (7). The line reproduces the linear increase with $R_\square$ seen in the data, and is in reasonable quantitative agreement as well. The line of unity slope that best fits the data lines about 20% higher than the solid line, and the scatter in the data is about ±20% around this best-fit line. Moreover, the fitted rates are in good agreement with rates from magnetoresistance measurements on similar films, extrapolated to T_c.[12–15]

We tried to fit the data with $\alpha^2F\propto\omega^1$ (Refs. 38–40) and $\alpha^2F\propto\omega^2$ (Ref. 41), which would correspond to normal-state scattering rates proportional to T^2 and T^3, respectively, but found that $\alpha^2F\propto\omega^0$ gave the best fit to R_j versus I_s with the most reasonable values of $1/\tau_{e\text{-}e}(T_c)$. Fits with the other forms for α^2F could be adjusted to give a possible fit, but the inflection points were always way off.

Given that the theory agrees well with the data, with physically reasonable values of the relevant parameters, it is interesting to use the theory to elucidate the very strong T dependence of the e-e scattering rate below T_c in contrast with that of e-phonon scattering and phase fluctuations. Unlike in the normal state, in the superconducting state there is no standard definition for characteristic scattering rates, so we need to improvise for this comparison. For the reasons outlined above, the inflection point in R_j versus $(1/\tau_{s,\text{ext}})^{1/2}$ is a reasonable measure of the effective intrinsic scattering rate in gen-

eral. By choosing one intrinsic rate much larger than the rest in the calculation, the inflection point reflects that one rate. Explicitly, from Eqs. (1)–(3), for temperatures near T_c, but far enough from T_c that the effect of extrinsic pair breaking on the energy gap is negligible, the inflection point should occur at $1/\tau_{s,\mathrm{ext}} \sim 1/2\tau_{\mathrm{int}}$, where $1/\tau_{\mathrm{int}} = 1/2\tau_{e\text{-}e} + 1/2\tau_{\mathrm{tun}} + 1/\tau_{\mathrm{SCF}}$ is the total intrinsic pair-breaking rate.

Results for the various scattering rates below T_c are shown in Fig. 7. The procedure for obtaining the curves is to solve the Boltzmann equation describing charge-imbalance generation and relaxation in the junction, and thence to calculate R_j versus $(1/\tau_{s,\mathrm{ext}})^{1/2}$, with the intrinsic pair breaking being due to *e-e* scattering (bottom curve); *e*-phonon scattering (middle curve); or phase fluctuations (top curve). The proximity effect contribution $1/2\tau_{\mathrm{tun}}$ to the total pair-breaking rate is unavoidable since the physical arrangement is a SIN junction. However, $1/2\tau_{\mathrm{tun}}$ is small so that the inflection point is determined primarily by the intrinsic rate of interest. The scattering rates in Fig. 7 are normalized so that the three curves would go to 0.5 at T_c if the strong dependence of Δ on $1/\tau_{s,\mathrm{ext}}$ did not cause the downturn seen very close to T_c. For the three curves, the total pair-breaking rate at T_c is the same, 2.8×10^8/s, which is much smaller than $\Delta(0)/\hbar$ so that $\Delta(T)$ and the density of states have their BCS values. For reference, all three curves merge at low temperatures where only the proximity-effect pair breaking remains and other processes freeze out.

Let us compare the curves in Fig. 7. When the dominant intrinsic charge-imbalance relaxing (pair-breaking) mechanism is elastic pair breaking associated with phase

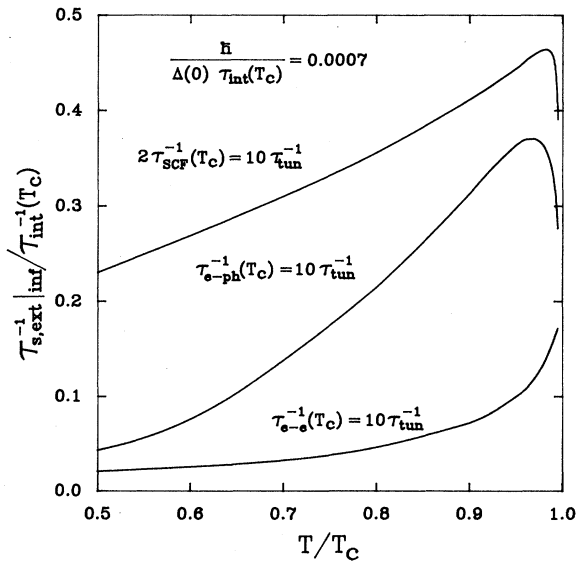

FIG. 7. $\tau_{s,\mathrm{ext}}^{-1}|_{\mathrm{infl}}/\tau_{\mathrm{int}}^{-1}(T_c)$ vs T/T_c for several different charge-imbalance relaxation processes. Notice the very sharp decrease of electron-electron scattering with decreasing T just below T_c.

fluctuations, then the effective pair-breaking rate measured by the inflection point in R_j versus $(1/\tau_{s,\mathrm{ext}})^{1/2}$ is roughly linear in T. When intrinsic pair breaking is due primarily to *e*-phonon scattering, with $\alpha^2F \propto \omega^2$ in the collision integral, then the effective rate decreases approximately as T^3, just as in the normal state. However, when the intrinsic pair breaking is due primarily to *e-e* scattering, with $\alpha^2F \propto \omega^0$, the effective rate decreases extremely rapidly just below T_c. From Fig. 7, it is clear why the *e-e* scattering and phase fluctuation rates can be separated on the basis of their different dependences on T.

There is an interesting physical reason for the rapid drop in the effective *e-e* scattering rate just below T_c. The reason concerns the number of bosons (damped plasmons), with sufficient energy to effectively relax a quasiparticle charge imbalance. Because α^2F is independent of energy, there are a very large number of low-energy bosons available to scatter. However, an excitation must change its energy by at least Δ in a scattering event if the event is to be effective in relaxing a charge imbalance because the coherence factor for charge-imbalance relaxation is zero for zero energy transfer, and increases to near unity only for energy transfers of about Δ. Thus as T decreases below T_c, and Δ increases rapidly, the number of thermal bosons with energy greater than Δ decreases exponentially with the Bose function, and so does the effective *e-e* scattering rate.

2. *Phase fluctuations*

The difference in the phase $\phi(\mathbf{r},t)$ of the order parameter $\Delta(\mathbf{r},t)$ between two nearby points in space develops in time according to the Josephson relation, $\partial\phi/\partial t = 2(eV + \mu)/\hbar$, where eV and μ are the electric and chemical potentials of the electrons, respectively. Fluctuations in the local electron density induce fluctuations in the electric potential V, and hence in ϕ. The fluctuations are also given in part by charge-imbalance fluctuations, i.e., fluctuations in the chemical potential μ.[42] Phase fluctuations are pair breaking because spatial gradients in the phase represent fluctuating supercurrents, which are pair breaking just as an applied supercurrent is. There exists at present no theory of disordered superconductors that includes phase fluctuations, although several authors have commented on the existence of phase fluctuations.[43–45] It would be useful and instructive to have such a theory to unify, clarify, and quantify the relationship between phase fluctuations and *e-e* scattering and their effects on superconductivity.

We include phase fluctuations in the theory the same way as an applied supercurrent, which is an elastic scattering term in the Boltzmann equation.[20] The temperature dependence of the associated pair-breaking rate is determined from the explicit T dependence of the amplitude of the fluctuations and the temperature and energy dependence of the relevant coherence factors and Fermi factors.

The magnitude of the pair-breaking rate from phase fluctuations can be estimated as follows. If all the superconducting electrons in a volume $\sim\xi^2(T)d$ undergo

Brownian motion as a single particle with the appropriate mass $mn_s\xi^2 d$, then the equipartition theorem gives the mean-square superfluid velocity $\overline{v_s^2}$ by $mn_s\xi^2 d\overline{v_s^2}/2 \simeq k_B T$, where $\overline{v_s^2}$ is a thermal average. The pair-breaking rate is calculated using Eq. (5) with $p_s^2=(2mv_s)^2$:

$$\frac{1}{\tau_{\rm SCF}^{\rm theor}(T)} \equiv \frac{\overline{1}}{\tau_s} \simeq \frac{4D}{\hbar^2}\frac{mk_B T}{n_s\xi^2(T)d} . \tag{9}$$

The important assumption here is that the size of the coherent particle is determined by the temperature-dependent coherence length $\xi(T)$.

A somewhat more microscopic approach, which gives the same result, is to consider each spatial Fourier component of the fluctuations independently.[46] The root-mean-square kinetic energy of each k mode is again determined by the equipartition theorem to be $k_B T/2$, i.e., $M_s\overline{v_{s,k}^2}/2=k_B T/2$, where M_s is the mass of all the superconducting electrons in the film since all superelectrons participate in each k mode. Since all the k modes are independent, we can calculate the net pair-breaking rate by summing $\overline{v_{s,k}^2}$ over k up to some cutoff, k_c. The choice $k_c \simeq 1/\xi(T)$ leads to Eq. (9). While this choice for k_c seems reasonable, the microscopic reason for this cutoff is not clear. Another reasonable choice is $1/\xi_P$, where ξ_P is the Pippard coherence length. In dirty films, $\xi_P \simeq l$ for all T. If there is no shorter cutoff, the cutoff surely occurs at $1/\xi_P$ because n_s is zero for k above $1/\xi_P$.[25]

A still more microscopic approach is to consider the Langevin equation for the fluctuating distribution of excitations in the superconductor, as was done by Aronov and Katilyus.[47] Even in that theory, the important question to be answered is, still, how is the pair-breaking effectiveness of a particular fluctuation k mode related to its wavelength?

The cutoff choice indicated by the data is that the size of the coherent particle is that of a Cooper pair, namely, the T-dependent Ginzburg-Landau coherence length. Near T_c, using dirty-limit expressions for $\xi(T)$ and $\lambda(T)$ (Ref. 25), Eq. (9) can be rewritten as

$$\frac{1}{\tau_{\rm SCF}^{\rm theor}(T)} \simeq 2.2\times 10^7 R_\square T , \tag{10}$$

in $(\Omega\,{\rm K\,s})^{-1}$. Note that Eq. (10) for $1/\tau_{\rm SCF}^{\rm theor}(T_c)$ is very similar to Eq. (7) for $1/\tau_{e\text{-}e}^{\rm theor}(T_c)$ in magnitude and dependence on $R_\square$ and T. The physical reason likely stems from the common origin of the two effects in electron-density fluctuations. The lower solid line in Fig. 5 was calculated from Eq. (10). Equation (10) is in reasonable quantitative agreement with the measured values of $1/\tau_{\rm SCF}(T_c)$, but describes a faster increase with $R_\square$ than is seen in the data. $1/\tau_{\rm SCF}(T_c) \propto R_\square^{2/3}$ fits the data much better. We do not understand the origin of this discrepancy.

In our numerical calculations, phase (supercurrent) fluctuations are included in the Boltzmann equation by simply adding the rate in Eq. (10) to the pair-breaking rate for applied supercurrents, as described in detail in Ref. 20. Although Eq. (10) is obtained near T_c, we have assumed that it is roughly valid at low T too, so that the pair-breaking rate vanishes at low temperatures. Figure 7 indicates that the contribution of phase fluctuations to charge-imbalance relaxation decreases roughly linearly in T when Eq. (10) is used.

This model can be extended to general dimensions[48] by replacing $\xi^2 d$ with $\xi^\delta d^{3-\delta}$ in Eq. (9), where δ is dimensionality and d is size of any dimension smaller than ξ. The result just below T_c is

$$\frac{1}{\tau_{\rm SCF}^{\rm theor}(T_c)} \simeq \frac{2D}{\hbar^2}\frac{\delta k_B T m}{n_s\xi^\delta(T)d^{3-\delta}} \sim \delta\times 10^7 T_c\frac{\rho}{d}\left[\frac{d}{\xi}\right]^{\delta-2} . \tag{11}$$

The rate increases with disorder for all three dimensionalities since $\rho \propto 1/l$ and $\xi \propto \sqrt{l}$. Also, the rate becomes larger in lower dimensions for a given material.

It is interesting to put phase fluctuations into the perspective of other work. In terms of Fourier components, phase fluctuations correspond to overdamped modes of oscillation, except in very restricted conditions of k and temperature. Very near T_c and for very large k values, fluctuations represent thermal excitation of Carlson-Goldman modes,[49] which are counteroscillations of superfluid and normal fluid such that the total electron density is constant. In very thin wires or films, for small k values, fluctuations represent thermal excitation of plasma modes described by Mooij and Schön[50] for narrow wires. For most k values, fluctuations are overdamped, and the pair-breaking effects of fluctuations are dominated by these damped modes. These latter authors noted the magnitude of fluctuation supercurrents associated with thermal excitation of plasma modes, but did not consider the contribution from damped modes. More details are in Ref. 46.

IV. CONCLUSION

We have performed measurements of the low-voltage resistance of low-resistance Al-AlO_x-Cu tunnel junctions as a function of temperature and of supercurrent both directly applied and induced by a magnetic field parallel to the film. Pair-breaking rates at T_c associated with electron-electron scattering and phase fluctuations are extracted from comparison of data with numerical calculations based on a Boltzmann-like theory of the quasiparticle distribution function, including both electron-electron scattering and phase fluctuations. Both pair-breaking processes are found to be enhanced by disorder and are described well by model calculations presented in this paper.

Measured values of the electron-electron scattering rate at T_c are in agreement with values from magnetoresistance measurements on similarly disordered Al films. Below T_c, the contribution of electron-electron scattering to charge-imbalance relaxation dropped very rapidly with decreasing T, in contrast to the linear T dependence predicted and observed above T_c, and in agreement with calculations. The measured pair-breaking rate from thermal phase fluctuations was in

reasonable agreement with a crude model calculation, but the model predicted a linear increase with $R_\square$, while the data fit better to $R_\square^{2/3}$. The pair-breaking rate from phase fluctuations decreased roughly linearly as T decreased.

More work is needed. Studying how the phase fluctuations are dynamically related to the formation of thermal vortex-antivortex pairs and KT transition in very disordered systems would be interesting. Also, since thermal phase fluctuations are believed to be enhanced in reduced dimensions, it would be interesting to study them in thin wires theoretically and experimentally. Electron-electron scattering and phase fluctuations are believed to be closely connected by a common driving force, electron-density fluctuations, but a microscopic theory is needed to verify and quantify this.

Finally, we comment on the experimental technique because of its novelty. The phenomenological parameter of interest here, the resistance R_j, is a linear-response transport parameter analogous to thermal and electrical conductivities because the first-order correction to the quasiparticle distribution function is important. A special feature of the technique is that it is sensitive only to pair-breaking rates, not simple elastic scattering unless the order parameter is anisotropic, and these rates are often of interest. Moreover, since the technique determines the relaxation *time*, it is especially sensitive to small rates, unlike conventional tunneling measurements that probe the pair-breaking *rate* from the broadening in the BCS singularity in the density of states. Also, in the dirty limit, the quasiparticle distribution function is isotropic in momentum space, simplifying the analysis. Disadvantages are that it involves fabrication of very low-resistance tunnel junctions on thin films and numerical solutions of the theory are tedious. However, in the end, the results presented here demonstrate the power of charge-imbalance measurements for studies of superconducting films.

ACKNOWLEDGMENTS

This work was supported by the National Science Foundation under Grant Nos. DMR-83-00254 and DMR-85-15370. One of us (T.R.L.) gratefully acknowledges support from the Alfred P. Sloan foundation. Also one of us (S.G.L.) gratefully acknowledges support from Ohio State University.

*Current address: IBM, Thomas J. Watson Research Center, Box 218, Yorktown Heights, NY 10598.

[1]S. G. Lee and T. R. Lemberger, Phys. Rev. B **37**, 7911 (1988).
[2]T. R. Lemberger and S. G. Lee, Physica B+C **153-155**, 1708 (1988).
[3]H. Raffy, R. B. Laibowitz, P. Chaudhari, and S. Maekawa, Phys. Rev. B **28**, 6607 (1983).
[4]J. M. Graybeal and M. Beasley, Phys. Rev. B **29**, 4167 (1984).
[5]A. F. Hebard and M. A. Paalanen, Phys. Rev. B **30**, 4063 (1984).
[6]A. F. Hebard and A. T. Fiory, Phys. Rev. Lett. **58**, 1131 (1987).
[7]P. Chaudhari, A. N. Broers, C. C. Chi, R. Laibowitz, E. Spiller, and J. Viggiano, Phys. Rev. Lett. **45**, 930 (1980).
[8]R. C. Dynes, J. P. Garno, and J. M. Rowell, Phys. Rev. Lett. **40**, 479 (1978).
[9]R. C. Dynes, J. P. Garno, G. B. Hertel, and T. P. Orlando, Phys. Rev. Lett. **53**, 2437 (1984).
[10]W. Eiler, J. Low Temp. Phys. **56**, 481 (1984).
[11]B. L. Altshuler, A. G. Aronov, and D. E. Khmelnitsky, J. Phys. C **15**, 7367 (1982).
[12]P. Santhanam, S. Wind, and D. E. Prober, Phys. Rev. Lett. **53**, 1179 (1984).
[13]P. Santhanam, S. Wind, and D. E. Prober, Phys. Rev. B **35**, 3188 (1987).
[14]J. M. Gordon, C. J. Lobb, and M. Tinkham, Phys. Rev. B **28**, 4046 (1983).
[15]J. M. Gordon and A. M. Goldman, Phys. Rev. B **34**, 1500 (1986).
[16]D. Belitz, Phys. Rev. B **35**, 1636 (1987).
[17]P. C. van Son, J. Romijn, T. M. Klapwijk, and J. E. Mooij, Phys. Rev. B **29**, 1503 (1984).
[18]T. M. Klapwijk, P. A. van der Plas, and J. E. Mooij, Phys. Rev. B **33**, 1474 (1986).
[19]Y. Yen and T. R. Lemberger, Phys. Rev. B **37**, 3324 (1988).
[20]T. R. Lemberger, Y. Yen, and S. G. Lee, Phys. Rev. B **35**, 6670 (1987).
[21]M. Tinkham, Phys. Rev. B **6**, 1747 (1972).
[22]T. R. Lemberger, Phys. Rev. B **29**, 4946 (1984).
[23]D. A. Browne, K. Levin, and K. A. Muttalib, Phys. Rev. Lett. **58**, 156 (1987).
[24]K. Maki, in *Superconductivity,* edited by R. D. Parks (Dekker, New York, 1969).
[25]See, for example, M. Tinkham, *Introduction to Superconductivity* (McGraw-Hill, New York, 1975).
[26]C. Kittel, *Introduction to Solid State Physics,* 5th ed. (Wiley, New York, 1976).
[27]D. E. Prober, in *Percolation, Localization, and Superconductivity,* Vol. 109 of *NATO Advanced Study Institute, Series B: Physics,* edited by A. M. Goldman and S. A. Wolf (Plenum, New York, 1984), p. 231.
[28]T. R. Lemberger, Phys. Rev. Lett. **52**, 1029 (1984).
[29]W. L. McMillan, Phys. Rev. **175**, 537 (1968).
[30]K. A. Gschneidner, Solid State Phys. **16**, 275 (1964).
[31]A. Schmid and G. Schön, J. Low Temp. Phys. **20**, 207 (1975).
[32]C. J. Pethick and H. Smith, Ann. Phys. (N.Y.) **119**, 133 (1979).
[33]J. Romijn, T. M. Klapwijk, M. J. Renne, and J. E. Mooij, Phys. Rev. B **26**, 3648 (1982).
[34]D. S. Pyun, E. R. Ulm, and T. R. Lemberger, Phys. Rev. B **39**, 4140 (1989).
[35]Y. Yen, S. G. Lee, and T. R. Lemberger, Phys. Rev. B **36**, 8408 (1987).
[36]C. C. Chi and J. Clarke, Phys. Rev. B **16**, 4495 (1979); **21**, 333 (1980).
[37]O. Entin-Wohlman and R. Orbach, Phys. Rev. B **31**, 5172 (1980).
[38]G. Bergmann, Phys. Rev. B **3**, 3797 (1971).
[39]H. Takayama, Z. Phys. **263**, 329 (1973).
[40]D. Belitz, Phys. Rev. B **36**, 2513 (1987).
[41]W. E. Lawrence and A. B. Meador, Phys. Rev. B **18**, 1154 (1978).

[42]T. R. Lemberger, Phys. Rev. B **24**, 4105 (1981).
[43]T. R. Lemberger, Physica B+C **107B**, 163 (1981).
[44]O. D. Cheishvili, J. Low Temp. Phys. **48**, 445 (1982).
[45]Y. Imry, Physica **55**, 344 (1971).
[46]S. G. Lee, Ph.D. thesis, Ohio State University, 1988 (unpublished).
[47]A. G. Aronov and R. Katilyus, Zh. Eksp. Teor. Fiz. **68**, 2208 (1975) [Sov. Phys.—JETP **41**, 1106 (1976)].
[48]T. R. Lemberger and S. G. Lee, in *Novel Superconductivity,* edited by S. A. Wolf and V. Z. Kresin (Plenum, New York, 1987), p. 83.
[49]R. V. Carlson and A. M. Goldman, Phys. Rev. Lett. **34**, 11 (1975).
[50]J. E. Mooij and G. Schön, Phys. Rev. Lett. **55**, 114 (1985).